Angewandte Chemie
Eine Zeitschrift der Gesellschaft Deutscher Chemiker

Supporting Information

69451 Weinheim, Germany

Elastic properties of photoswitchable azobenzene polymers from molecular dynamics simulations

Lars V. Schäfer, E. Matthias Müller, Hermann E. Gaub, and Helmut Grubmüller

Simulation Details

Setup

All simulations were carried out with the Gromacs simulation suite[1] using the OPLS all-atom force field[2] and periodic boundary conditions. NpT ensembles were simulated, with the polymer and solvent separately coupled to a 300 K heat bath ($\tau_T = 0.1$ ps).[3] The systems were isotropically coupled to a 1-bar pressure bath ($\tau_p = 1.0$ ps).[3] Application of the Lincs[4] algorithm allowed for an integration time step of 2 fs. Short-range electrostatic and Lennard-Jones interactions were calculated within a cutoff of 1.0 nm and 1.4 nm, respectively, and the neighbor list was updated every 10 steps. The Particle-Mesh-Ewald (PME) method was used for the long-range electrostatic interactions.[5] To compensate for the net positive charge of the protonated polymers, four chloride ions were added.

The OPLS force constants of the angles involving the central azo-moiety are crucial for the elastic properties of azobenzene and were therefore determined using accurate quantum chemical calculations. To this end, relaxed potential energy surface scans along a stretching coordinate (distance of the azobenzene *p*-carbon atoms) were performed in vacuo at the B3LYP/6-311+G* density functional level[6, 7] using Gaussian03.[8] As shown in the Supporting Information, Fig. 1, the OPLS parameters were chosen such as to accurately match the quantum chemical calculations concerning both, (i) the potential energy along the stretching coordinate, and (ii) the corresponding structures. Atomic partial charges of azobenzene were obtained from B3LYP/6-31G* calculations according to the CHELPG scheme.[9] The employed force field parameters are summarized in the tables below.

The starting configurations for the FPMD simulations were obtained as follows. First, the azobenzene polymers were constructed using pymol.[10] In these structures, the lysines and glycines were modeled in their extended anti conformations, with ψ and φ backbone dihedral angles of 135° and -140°, respectively. Second, the polymers were solvated in a cubic box of DMSO and energy minimized (1000 steps steepest descent), followed by 500 ps of MD with positional restraints on all polymer heavy atoms to equilibrate the solvent. Then, the whole system was equilibrated for 1 ns, after which the solvent was removed. The polymer was aligned along the box *z*-axis, which was extended to enable the accommodation of the fully stretched conformation. Finally, DMSO was added to this elongated box and equilibrated with positional restraints on all

polymer heavy atoms for another 500 ps to yield the starting configurations for the FPMD simulations. Depending on the capping of the lysine side chains and the azobenzene conformations, total system sizes were between 35,000 and 57,000 atoms.

Force Probe MD Simulations

The N-terminus, N_α, was subjected to a moving harmonic spring potential,

$$V_{spring,N_\alpha}(t) = k_0 \left[z_{N_\alpha}(t) - z_{spring}(t)\right]^2,$$

where $k_0 = 500\,\mathrm{kJ\ mol^{-1}nm^{-2}}$ is the force constant of the spring, $z_{N\alpha}(t)$ is the position of the pulled N_α atom, and $z_{spring}(t)$ the position of the spring. The C-terminus, C_ω, was fixed by a stationary harmonic potential ($k_{fix} = 1000\,\mathrm{kJ\ mol^{-1}nm^{-2}}$). Mechanical stress to probe the elastic behavior of the model polymers was applied by moving the spring with constant velocity v in positive z-direction, $z_{spring}(t) = z(0) + vt$, with $z(0) := z_{N_\alpha}(0)$. During the FPMD simulations, z_{spring}, z_{N_α}, and the position of the C-terminus were recorded every 0.1 ps, whereas the positions of all polymer atoms were recorded every 0.5 ps. For further analysis, the force at the spring potential was averaged using a 50 ps time window. The data for the WLC fits were truncated at 500 pN, as the maximally achievable force in the AFM experiments.

FPMD simulations were carried out with pulling velocities of $v = 0.1$ nm/ns and $v = 0.5$ nm/ns, yielding simulation times of 50 to 70 ns and 10 to 14 ns per FPMD trajectory, respectively (Table I). The overall simulation time was about 0.5 microseconds.

Controls

Because the chemistry of the lysine side chains of the polymers used in the AFM experiments could not be unambiguously established, we repeated the simulations of the dodecamer with (i) all lysine side chains charged, and (ii) all lysine side chains capped with an adamanyl-oxycarbonyl protection group (Adoc). Thus, taken together with the uncharged model polymer described above, the lysine side chains were modeled in all conceivable ways. The WLC parameters (Table I) show that the elastic properties of the charged and Adoc-capped model systems do not differ significantly from the uncharged model polymer. As we will detail below, this is because the elastic behavior is dominated by the polymer backbone, and not by the side chains.

system	$\Delta l/monomer$ (Å)	$L_c/monomer$ (nm)	L_p (nm)	R^2_{free}	R^2_{fix}
experiment (Ref. [11])	0.60	1.90	0.50		
uncharged, $v = 0.1$ nm/ns	1.45	2.05	0.97	0.88	0.85
uncharged, $v = 0.5$ nm/ns (sim 1)	1.48	2.07	0.68	0.92	0.91
uncharged, $v = 0.5$ nm/ns (sim 2)	1.49	2.12	0.40	0.89	0.88
charged, $v = 0.5$ nm/ns	1.34	2.11	0.41	0.92	0.92
Adoc-capped, $v = 0.5$ nm/ns	1.38	2.10	0.45	0.87	0.87

Table I: WLC parameters of all-trans polymers obtained from experiment and from our FPMD simulations, obtained by fitting the force-extension data to the extended WLC model (Eq. **??**). The extension difference Δl per switched azobenzene monomer is given at a force of 200 pN to enable direct comparison to the experiment. Two different values are given for R^2, reflecting the quality of the fits. R^2_{free} was obtained from a WLC fit with both, L_c and L_p as adjustable parameters, whereas R^2_{fix} was obtained from a fit with $L_p = 0.5$ nm, which is the value obtained from the experimental data.

To test the influence of the pulling velocity on the elastic properties, we carried out two independent FPMD simulations of the $(Lys-Azo-Gly)_4$ dodecamer at a five times faster pulling velocity of 0.5 nm/ns. Both simulations yielded similar results. The overall and individual force-extension curves as well as the analysis of the ψ backbone dihedral angle for one of the simulations are shown in Figures 3, 4, and 5, respectively; the results of the WLC fits are shown in Table I. The elastic properties obtained from these simulations closely match those from the simulations at the slower pulling velocity of 0.1 nm/ns. Thus, we consider the structural dynamics underlying the elastic properties of the polymers to be correctly captured already at the faster pulling velocity.

The reversibility of forward and backward pulling serves as an additional check that the system is sufficiently close to equilibrium at all times for the used pulling velocity. Starting from the fully extended configuration of the all-cis model polymer, a simulation with reversed pulling direction was carried out. As evident from Fig. 6, there is virtually no hysteresis between the forward and backward force-extension traces obtained at $v = 0.5$ nm/ns, showing that the system was indeed close to equilibrium during the simulation.

To study finite size effects, we carried out FPMD simulations of a model system containing three instead of four azotripeptide units, $(Lys-Azo-Gly)_3$, at a pulling velocity of 0.1 nm/ns.

Here, only the all-cis and all-trans models were simulated. The overall and individual force-extension curves are shown in Figures 7 and 8, respectively. The elastic properties of the shorter nonameric polymer are similar to those of the dodecamer ($L_c = 2.08\,\mathrm{nm}$ and $L_p = 0.59\,\mathrm{nm}$). Also in the shorter system, the lysines partly compensate the azobenzene contraction upon optical switching. Since these features, which dominate the mechanics of the dodecamers are also seen in the shorter nonamer, we consider the dodecameric model polymer sufficiently large and finite size effects negligible.

To rule out aggregation of azobenzene moieties during the AFM experiments due to non-covalent interactions, the molecular weight of the polymers was determined (Ref. [11], supplementary material). An average contour length of 80 to 100 nm was obtained. After coupling the polymers to the tip (via the cysteine group) and to the waveguide (via the carboxyl group), the same contour length was found in the single molecule optomechanical experiments. Since, furthermore, the lateral density of the grafting points was kept very low, interaction between individual polymers can be neglected in the experiments.

---

[1] D. van der Spoel, B. Hess, E. Lindahl, G. Groenhof, A. E. Mark, H. J. C. Berendsen, *J. Comput. Chem.* **2005**, *26*, 1701.

[2] W. L. Jorgensen, J. Tirado-Rives, *J. Am. Chem. Soc.* **1988**, *110*, 1657.

[3] H. J. C. Berendsen, J. P. M. Postma, W. F. van Gunsteren, A. DiNola, J. R. Haak, *J. Chem. Phys.* **1984**, *81*, 3684.

[4] B. Hess, H. Bekker, H. J. C. Berendsen, J. G. E. M. Fraaije, *J. Comp. Chem.* **1997**, *18*, 1463.

[5] T. Darden, D. York, L. Pedersen, *J. Chem. Phys.* **1993**, *98*, 10089.

[6] A. D. Becke, *Phys. Rev. A* **1988**, *38*, 3098.

[7] C. T. Lee, W. T. Yang, R. G. Parr, *Phys. Rev. B* **1988**, *37*, 785.

[8] M. J. Frisch, G. W. Trucks, H. B. Schlegel, G. E. Scuseria, M. A. Robb, J. R. Cheeseman, J. A. Montgomery, Jr., T. Vreven, K. N. Kudin, J. C. Burant, J. M. Millam, S. S. Iyengar, J. Tomasi, V. Barone, B. Mennucci, M. Cossi, G. Scalmani, N. Rega, G. A. Petersson, H. Nakatsuji, M. Hada, M. Ehara, K. Toyota, R. Fukuda, J. Hasegawa, M. Ishida, T. Nakajima, Y. Honda, O. Kitao, H. Nakai, M. Klene, X. Li, J. E. Knox, H. P. Hratchian, J. B. Cross, V. Bakken, C. Adamo, J. Jaramillo, R. Gomperts, R. E. Stratmann, O. Yazyev, A. J. Austin, R. Cammi, C. Pomelli, J. W. Ochterski, P. Y. Ayala, K. Morokuma,

G. A. Voth, P. Salvador, J. J. Dannenberg, V. G. Zakrzewski, S. Dapprich, A. D. Daniels, M. C. Strain, O. Farkas, D. K. Malick, A. D. Rabuck, K. Raghavachari, J. B. Foresman, J. V. Ortiz, Q. Cui, A. G. Baboul, S. Clifford, J. Cioslowski, B. B. Stefanov, G. Liu, A. Liashenko, P. Piskorz, I. Komaromi, R. L. Martin, D. J. Fox, T. Keith, M. A. Al-Laham, C. Y. Peng, A. Nanayakkara, M. Challacombe, P. M. W. Gill, B. Johnson, W. Chen, M. W. Wong, C. Gonzalez, J. A. Pople Gaussian, Inc., Wallingford, CT, 2004.

[9] C. M. Breneman, K. B. Wiberg, *J. Comput. Chem.* **1990**, *11*, 361.

[10] W. L. DeLano, *The PyMOL Molecular Graphics System on World Wide Web http://www.pymol.org* **2002**.

[11] T. Hugel, N. B. Holland, A. Cattani, L. Moroder, M. Seitz, H. E. Gaub, *Science* **2002**, *296*, 1103.

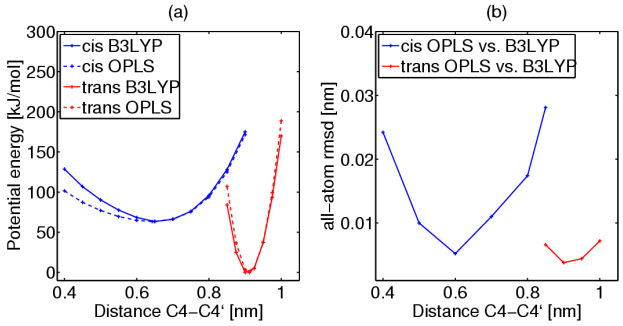

Figure 1: Parametrization of OPLS force field using B3LYP/6-311+G* density functional calculations. (a) Potential energy along the C4-C4' stretching coordinate of azobenzene in vacuo. The curves for cis and trans azobenzene are shown in blue and red, respectively. The OPLS force field was parametrized such that the force field potential energy (dashed lines) closely match the B3LYP/6-311+G* energy (solid lines). The energy difference between cis and trans was taken from the DFT calculation. Note that cis azobenzene is significantly softer as compared to trans. (b) all-atom rmsd between the force field and DFT structures along the stretching coordinate.

Figure 2: Schematic drawing of azotripeptide defining the decomposition into individual building blocks. The lysine, azobenzene, and glycine residues are shown in orange, green, and black, respectively. Note that the boundaries of the residues are different from the 'chemical boundaries' defined by the amide bonds, such that the azobenzene is solely defined by the N=N moiety plus the phenyl rings.

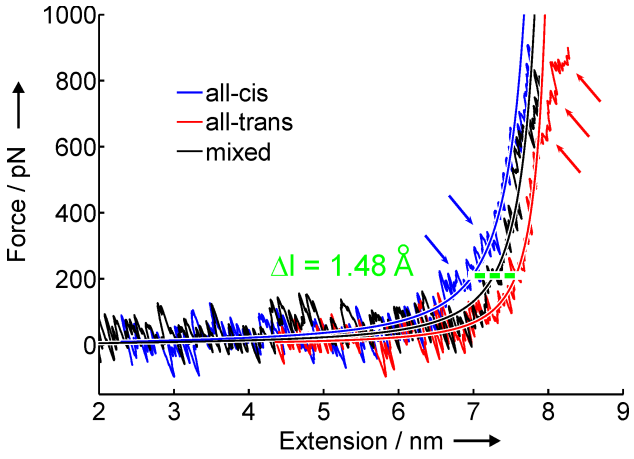

Figure 3: FPMD force-extension curves obtained at a pulling velocity of 0.5 nm/ns. The extension is defined as the distance between the C- and N-terminus of the polymer along the pulling direction. The curves for the all-cis, all-trans, and mixed polymers are shown in blue, red, and black, respectively. The data underlying the WLC fits (solid lines) were truncated at a force of 500 pN.

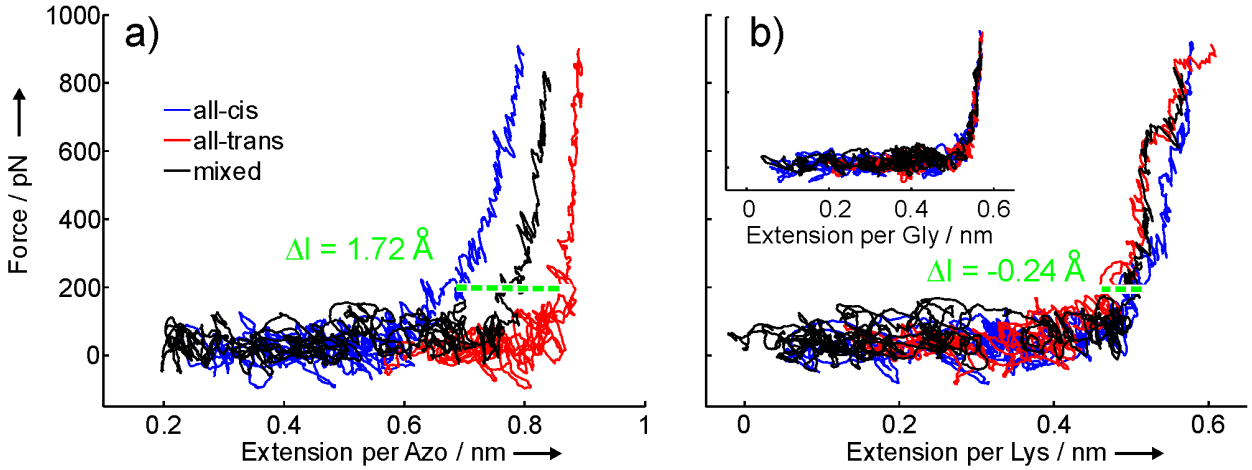

Figure 4: Force-extension curves of individual residues obtained at a pulling velocity of 0.5 nm/ns. (a) Average extension of azobenzenes. (b) Average extension of lysines and glycines (inset). The curves for the all-cis, all-trans, and mixed cis-trans-cis-trans dodecamers are shown in blue, red, and black, respectively.

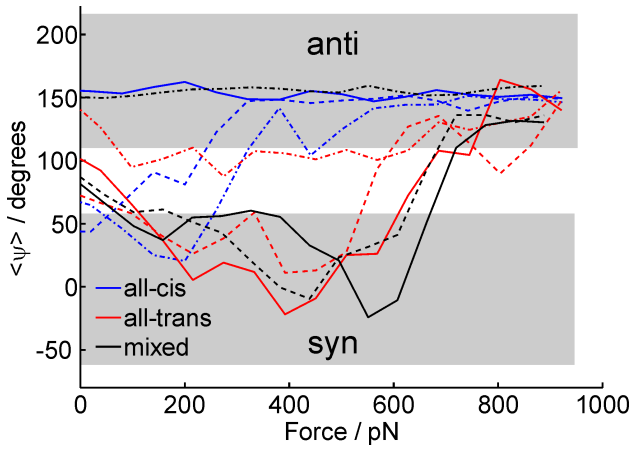

Figure 5: The average of the ψ dihedral angle is plotted as a function of the applied force for Lys4 (solid), Lys7 (dash-dotted), and Lys10 (dashed lines) of the all-cis (blue), all-trans (red), and mixed (black) polymers. The force was obtained at a pulling velocity of 0.5 nm/ns.

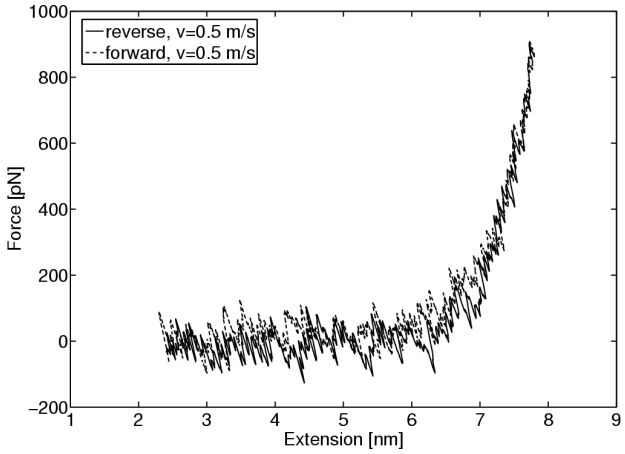

Figure 6: Forward (dashed line) and backward (solid line) FPMD force-extension curves of the all-cis polymer, obtained at a pulling velocity of 0.5 nm/ns. At this pulling velocity, there is virtually no hysteresis between the forward and backward directions, and thus the stretching is fully reversible.

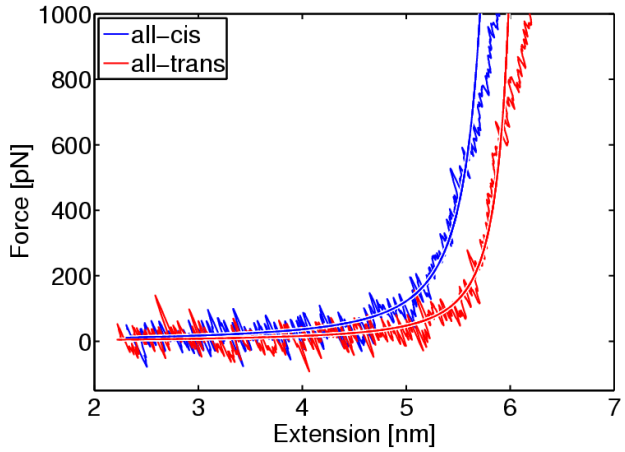

Figure 7: FPMD force-extension curves for the nonamer $(Lys-Azo-Gly)_3$, obtained at a pulling velocity of 0.1 nm/ns. The curves for the all-cis and all-trans systems are shown in blue and red, respectively.

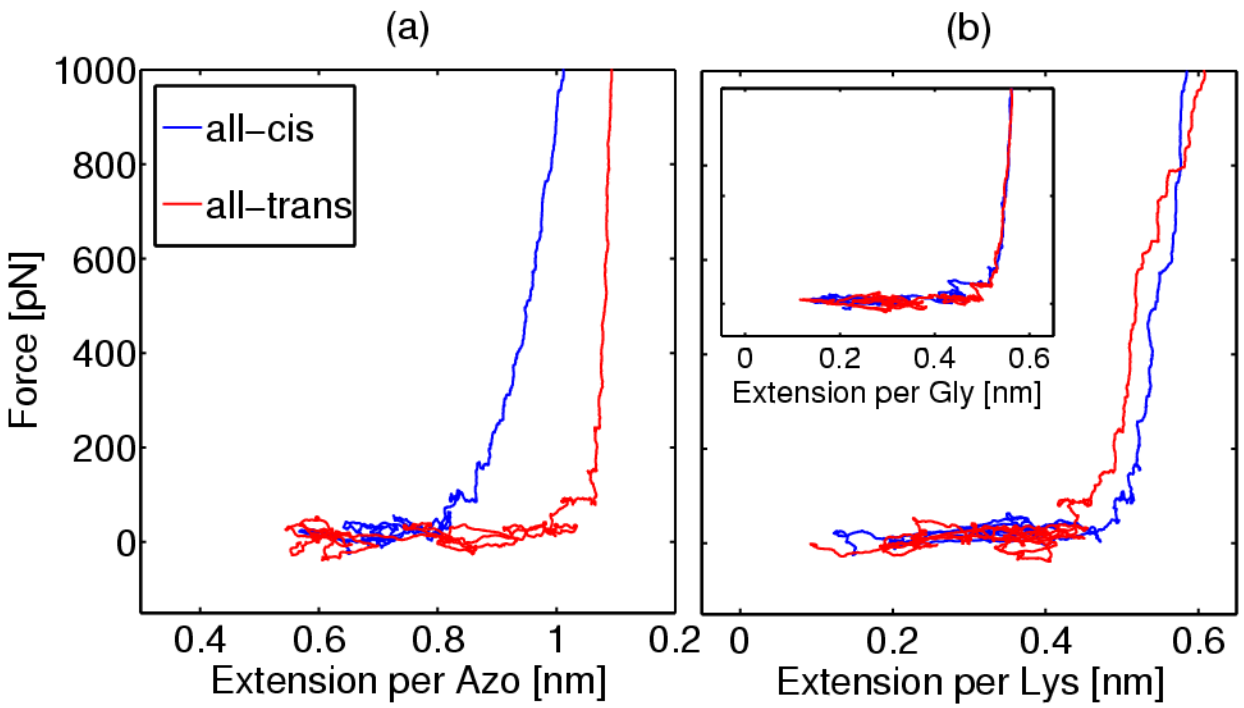

Figure 8: Force-extension curves of individual residues of the nonamer, obtained at a pulling velocity of 0.1 nm/ns. (a) Average extension of azobenzenes. (b) Average extension of lysines and glycines (inset). The curves for the all-cis, all-trans, and mixed dodecamers are shown in blue, red, and black, respectively.

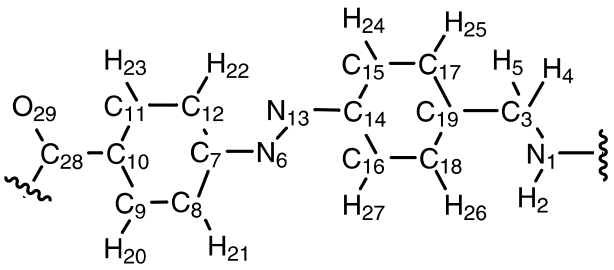

Figure 9: Schematic drawing of azobenzene, defining the atom names used in the Tables.

#	OPLS type	Atom type	q(cis)	q(trans)
1	opls_238	N	-0.50	-0.50
2	opls_241	H	-0.30	-0.30
3	opls_223B	CT_2	0.14	0.14
4	opls_140	HC	0.03	0.03
5	opls_140	HC	0.03	0.03
6	opls_998 / 999	NAC / NAT	-0.28	-0.22
7	opls_145 / 997	CA / CAT	0.53	0.34
8	opls_145 / 997	CA / CAT	-0.33	-0.10
9	opls_145 / 997	CA / CAT	-0.02	-0.09
10	opls_145 / 997	CA / CAT	-0.14	-0.13
11	opls_145 / 997	CA / CAT	-0.02	-0.03
12	opls_145 / 997	CA / CAT	-0.33	-0.21
13	opls_998 / 999	NAC / NAT	-0.28	-0.22
14	opls_145 / 997	CA / CAT	0.53	0.34
15	opls_145 / 997	CA / CAT	-0.33	-0.10
16	opls_145 / 997	CA / CAT	-0.33	-0.21
17	opls_145 / 997	CA / CAT	-0.02	-0.09
18	opls_145 / 997	CA / CAT	-0.02	-0.03
19	opls_145 / 997	CA / CAT	0.04	0.07
20	opls_146	HA	0.09	0.10
21	opls_146	HA	0.16	0.05
22	opls_146	HA	0.16	0.05
23	opls_146	HA	0.09	0.09
24	opls_146	HA	0.16	0.10
25	opls_146	HA	0.09	0.09
26	opls_146	HA	0.09	0.10
27	opls_146	HA	0.16	0.05
28	opls_235	C	0.50	0.50
29	opls_236	O	-0.50	-0.50

Table III: Atomic charges. Entries in the “OPLS type” and “Atom type” columns before and after the slash refer to cis and trans azobenzene, respectively.

OPLS type	Atom type	V	W
opls_997	CAT	0.355	0.293076
opls_998	NAC	0.325	0.711756
opls_999	NAT	0.325	0.711756

Table V: Lennard-Jones (6,12) parameters used in the OPLS force field.

Atom type	Atom type	b_0, nm	f_c, kJ/mol/nm^2
NAC	NAC	0.134	459710.6
NAT	NAT	0.118	459710.6
CA	NAC	0.143	357552.7
CA	NAT	0.140	357552.7

Table VII: Equilibrium bond lengths and force constants used in the OPLS force field.

Atom type	Atom type	Atom type	θ_0, deg	f_c,kJ/mol/rad^2
CA	CA	NAC	124.0	586.152
CA	NAC	NAC	115.0	427.0
CAT	CAT	NAT	124.0	586.152
CAT	NAT	NAT	108.0	1000.0
CAT	CAT	CAT	120.0	700.0
CA	CA	CA	120.0	527.537
N	CT_2	CA	114.0	527.184
N	CT_2	CAT	114.0	527.184
CA	CT_2	N	114.0	527.184
CAT	CT_2	N	114.0	527.184
CT_2	CA	CA	120.0	585.760
CT_2	CAT	CAT	120.0	585.760
HC	CT_2	CA	109.5	292.880
HC	CT_2	CAT	109.5	292.880

Table IX: Equilibrium angles and force constants used in the OPLS force field.

Atom type	Atom type	Atom type	Atom type	C_0, kJ/mol	C_1, kJ/mol	C_2, kJ/mol	C_3, kJ/mol
NAC	NAC	CA	CA	16.038	-4.394	-14.394	2.395
CA	NAC	NAC	CA	100.0	0	-100.0	0
NAC	CA	CA	CA	30.354	0	-30.354	0
NAC	CA	CA	HA	30.354	0	-30.354	0
NAT	NAT	CAT	CAT	16.038	-4.394	-14.394	2.395
CAT	NAT	NAT	CAT	100.0	0	-100.0	0
NAT	CAT	CAT	CAT	30.354	0	-30.354	0
NAT	CAT	CAT	HA	30.354	0	-30.354	0
CAT	CAT	CAT	CAT	30.354	0	-30.354	0
CAT	CAT	CAT	HA	30.354	0	-30.354	0
HA	CAT	CAT	HA	30.354	0	-30.354	0
CAT	CAT	CAT	C	30.354	0	-30.354	0
HA	CAT	CAT	C	30.354	0	-30.354	0
CAT	CAT	C	O	8.782	0	-8.792	0
CAT	CAT	CAT	CT_2	30.354	0	-30.354	0
HA	CAT	CAT	CT_2	30.354	0	-30.354	0
CAT	CAT	C	N	4.605	0	-4.605	0

Table XI: Ryckaert-Bellemans dihedral parameters used in the OPLS force field; C_4 and C_5 were zero in all cases and thus are not listed.